Non-average Stability Analysis for a Boost Converter

ANDRES GARCIA, EDUARDO GUILLERMO
GESE, Departamento de Ingeniería Eléctrica,
Universidad Tecnológica Nacional. Facultad Regional Bahía Blanca,
11 de abril 461, Bahía Blanca, Buenos Aires,
ARGENTINA

Abstract: - The purpose of this paper is to present a method for analyzing the stability of DC-DC boost converters providing a universal transfer function. This method relies on the application of the Laplace transform without any ad-hoc linear approximation or system linearization. A common methodology for evaluating the stability of DC-DC converters is the average method, which is essentially a linearization. In this paper, the Laplace transform is applied directly, resulting in a universal Z-transform model being used to design controllers and stability analyses as a discrete unifying transfer function. The examples cover both power and low voltage converters. Matlab simulations have been conducted to verify the theoretical findings. In particular, the second example considers a small 5V to 12V boost converter, which was previously examined in a Texas Instruments application note. The transfer functions and the Bode plot are provided.

Key-Words: - Power converters, Z-transform, Stability analysis, Average model, Switching model, Boost converter, State-Space.

Received: March 7, 2023. Revised: December 5, 2023. Accepted: December 21, 2023. Published: December 31, 2023.

1 Introduction

Renewable energy technologies always search for new and optimized DC-DC battery chargers and also DC-AC converters, [1]. While the well-known DC-DC buck is well studied and the design process is straightforward, for DC-DC boost converters, the case is of a much more complex nature, proving in general to be an unstable system, [2], [3].

One of the main limitations in the analysis and design of control algorithms and techniques for closed-loop stabilization of DC-DC converters lies on its switching nature, [4]. Unlike linear and non-linear continuous control systems, switching systems, even piecewise-linear ones, offer a very challenging control scenario, [5].

For this reason, the well-known average method was introduced in the late 70s as a method to obtain a linearized version of switching DC-DC converters as a unique transfer function, [6], [7]. With a clear advantage of having a unique model, continuous and time-invariant. However, the great disadvantage of this method lies in its local and linearized nature, not allowing for a ripple of heavy transient analysis, [8].

On the other hand, the available literature about boost converter control makes use of switching models either applying Laplace transform and then applying Z-transform or working with switching transfer functions, besides non-linear and complex control techniques, [9], [10].

In this paper, considering an asynchronous boost converter topology, under the assumption that the inductor's current is complementary to the switching MOS-FET current: when the inductor is charged, the switching is in on-mode and vice versa. In the same manner, the diode's current is complementary and is in line with the inductor's one: both conduct current to the load at the same time.

The remainder of the paper is organized as follows:
Section 2 presents the main theorem and its corollary to harvest and obtain a true transfer function without linearization and applying Laplace's ttransform to a given power converter: DC-DC or DC-AC, Section [Matlab] applies the results to the well-known boost converter to design a lead compensator providing stability along with some Matlab simulations using the Power Systems toolbox in Simulknk. Finally, Section [Conclusions] depicts some conclusions and future work.

2 The Boost Converter's Model

The most common asynchronous DC-DC Boost converter topology is shown in Figure 1.

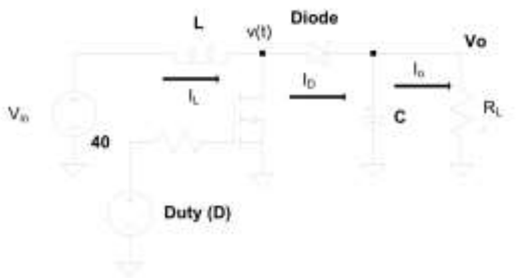

Fig. 1: Asynchronous boost converter topology

As it is well known, the PWM signal is the control modeled as a duty $D \in [0,1]$ variation. Therefore, the electrical equations can be modelled to be:

$$\begin{cases} I_D = (1-\delta(t)) \cdot I_L(t) \\ I_D = I_C + I_o \end{cases} \quad (1)$$

Where the PWM signal is modeled as $\delta(t)$ as shown in Figure 2 and the inductance's current is modeled to be complementary to the diode's current.

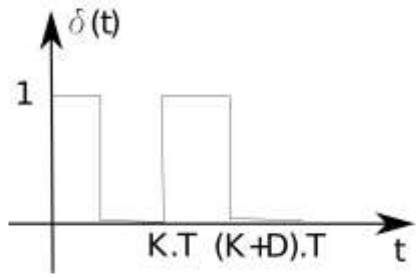

Fig. 2: PWM signal $\delta(t)$

Using a resistive load R_L along with the capacitor's law, Kirchoff's law (1) can be transformed to be:

$$\begin{cases} (1-\delta(t)) \cdot I_L(t) = C \cdot \dot{v}_o + \frac{v_o}{R_L} \\ -\frac{V_{in} - v(t)}{L} = \dot{I}_L \\ v(t) = (1-\delta(t)) \cdot V(D) \end{cases} \quad (2)$$

Where $V(D)$ is a constant voltage depending on the duty D. In the case of boost converters:

$$V(D) = \frac{V_{in}}{1-D} \quad (3)$$

defining a current control scheme over the inductance's current I_L, the complete model, plugging (3) into (2) yields:

$$\begin{cases} (1-\delta(t)) \cdot I_L(t) = C \cdot \dot{v}_o + \frac{v_o}{R_L} \\ -\frac{V_{in} - (1-\delta(t)) \cdot \frac{V_{in}}{1-D}}{L} = \dot{I}_L \\ y(t) = I_L(t) \end{cases} \quad (4)$$

In the next subsections, a complete, non-linearized model is developed using the Laplace transform considering an internal voltage as an auxiliary input variable parametrized by the duty D.

3 Output Stage Modelling

It is worth to develop a separate Laplace's transform analysis for the output voltage v_o using the voltage source $v(t)$ as shown in Figure 3.

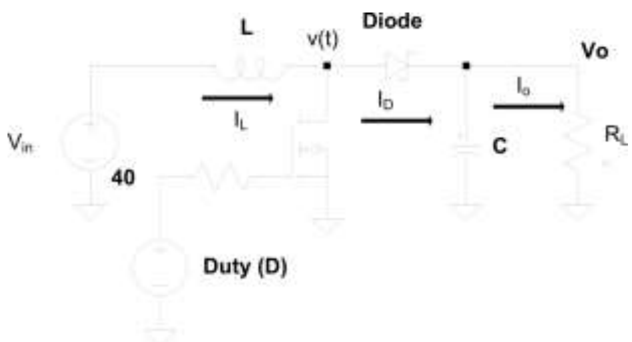

Fig. 3: Output circuit

Then, it is clear the two-stage switching equations:

$$\delta(t) = 1 \quad \text{discharge} \begin{cases} -C \cdot \dot{v}_0(t) = \frac{v_o}{R_L} \\ v_o(0) = V(D) \quad \text{Previous: charge} \end{cases}$$

$$\delta(t) = 0 \quad \text{charge} \begin{cases} \dot{v}_0(t) = -\left(\frac{1}{R_D} + \frac{1}{R_L}\right) \cdot \frac{1}{C} \cdot v_o + \frac{1}{R_D \cdot C} \cdot V(D) \\ R_D \quad \text{diode modeled as a resistance} \\ v_o(0) = e^{-\frac{1}{R_L \cdot C} \cdot (1-D) \cdot T} V(D) \quad \text{Previous: discharge} \end{cases}$$

Finally:

$$v_o(t) = (1-\delta(t)) \cdot \left[e^{-a \cdot t} \left(v_o(0) - \frac{V(D)}{\frac{R_D}{R_L}+1} \right) + \frac{V(D)}{\frac{R_D}{R_L}+1} \right] + \delta(t) \cdot V(D) \cdot e^{-\frac{1}{R_L \cdot C} \cdot t} \quad (5)$$

Where $a = \left(\frac{1}{R_L} + \frac{1}{R_D}\right) \cdot \frac{1}{C}$. Next subsection groups this output equation along with the boost's circuit equations (4).

4 The Complete Model in the s and z Domains

4.1 $I_L(s)$

Taking Laplace's transform on model (4) along with the output equations (5):

$$\begin{cases} \mathcal{L}\{(1-\delta(t))\cdot I_L(t)\} = \mathcal{L}\{C\cdot \dot{v}_o + \frac{v_o}{R}\} \\ \mathcal{L}\{\frac{V_{in}-(1-\delta(t))\cdot V(D)}{L}\} = \mathcal{L}\{\dot{I}_L\} \\ \mathcal{L}\{y(t)\} = \mathcal{L}\{I_L(t)\} \end{cases} \quad (6)$$

Where $\mathcal{L}\{f(t)\}$ means the Laplace's transform. Then, the focus is on $\mathcal{L}\{1-\delta(t)\cdot I_L(t)\}$:

$$\mathcal{L}\{(1-\delta(t))\cdot I_L(t)\} = \sum_{k=0}^{\infty}\int_{(K+D)\cdot T}^{(K+1)\cdot T} e^{-s\cdot t}\cdot I_L(t)\cdot dt$$

According to (4): $-\frac{V_{in}-(1-\delta(t))\cdot V(D)}{L} = \dot{I}_L$ and integrating by parts:

$$\mathcal{L}\{(1-\delta(t))\cdot I_L(t)\}(s) = \sum_{k=0}^{\infty}\left[-I_L(t)\cdot\frac{e^{-s\cdot t}}{s}\Big|_{(K+D)\cdot T}^{((K+1)\cdot T)} + -\int_{(K+D)\cdot T}^{(K+1)\cdot T}\frac{e^{-s\cdot t}}{s}\cdot\left(\frac{V_{in}-(1-\delta(t))\cdot V(D)}{L}\right)\cdot dt\right]$$

Taking into account the definition of $\delta(t)$:

$$\int_{(K+D)\cdot T}^{(K+1)\cdot T}\frac{e^{-s\cdot t}}{s}\cdot\delta(t)\cdot\frac{V(D)}{L}\cdot dt = 0$$

Then:

$$\mathrm{L}\{1-\delta(t)\cdot I_L(t)\}(s) = -\sum_{K=0}^{\infty}\left[I_L((K+1)\cdot T)\cdot\frac{e^{-s\cdot(K+1)\cdot T)}}{s}\right] + \\ +\sum_{K=0}^{\infty}\left[I_L((K+D)\cdot T)\cdot\frac{e^{-s\cdot(K+D)\cdot T}}{s} + \\ +\int_{(K+D)\cdot T}^{(K+1)\cdot T}\frac{e^{-s\cdot t}}{s}\cdot\frac{(V_{in}-V(D))}{L}\cdot dt\right]$$

Considering high frequency switching, the following assumption will be used along the paper:

Assumption 1: $T\to 0$, then: $I_L((K+D)\cdot T)\sim I_L(K\cdot T)$.

In this way:

$$\mathcal{L}\{1-\delta(t)\cdot I_L(t)\}(s) = \\ = -\sum_{k=0}^{\infty}\left[I_L((K+1)\cdot T)\cdot\frac{e^{-s\cdot(K+1)\cdot T)}}{s}\right] + \\ +\sum_{k=0}^{\infty}\left[I_L(K\cdot T)\cdot\frac{e^{-s\cdot(K+D)\cdot T)}}{s} + \\ -\int_{(K+D)\cdot T}^{(K+1)\cdot T}\frac{e^{-s\cdot t}}{s}\cdot\frac{V_{in}}{L}\cdot dt + \\ +\int_{(K+D)\cdot T}^{(K+1)\cdot T}\frac{e^{-s\cdot t}}{s}\cdot\delta(t)\cdot\frac{V(D)}{L}\cdot dt\right]$$

This infinite sum involving exponentials is exactly the definition of the Z-transform replacing $e^{s\cdot T} = z$, [11]:

$$\mathcal{L}\{1-\delta(t)\cdot I_L(t)\}(s) = \\ = -\sum_{k=0}^{\infty}\left[I_L((K+1)\cdot T)\cdot\frac{z^{-(K+1)}}{s}\right] + \\ \sum_{k=0}^{\infty}\left[I_L(K\cdot T)\cdot\frac{e^{-s\cdot(K+D)\cdot T)}}{s} + \\ -\int_{(K+D)\cdot T}^{(K+1)\cdot T}\frac{e^{-s\cdot t}}{s}\cdot\frac{V_{in}}{L}\cdot dt + \\ +\int_{(K+D)\cdot T}^{(K+1)\cdot T}\frac{e^{-s\cdot t}}{s}\cdot\delta(t)\cdot\frac{V(D)}{L}\cdot dt\right]$$

Moreover, recalling the formal definition of the Z-transform: $Z\{x(t)\}(z) = \sum_{K=0}^{\infty} x((K+1)\cdot T)\cdot z^{-K}$ along with the change of variables $K^* = K+1$, yields:

$$\mathcal{L}\{1-\delta(t)\cdot I_L(t)\}(s) = -Z\{I_L(t)\}(z)\cdot\frac{z^{-1}}{s} + \\ I_L(0)\cdot\frac{z^{-1}}{s} + Z\{I_L(t)\}(z)\cdot\frac{z^{-D}}{s} + \\ -\sum_{k=0}^{\infty}\frac{(V_{in}-V(D))}{L\cdot s^2}\cdot e^{-s\cdot t}\Big|_{(K+D)\cdot T}^{(K+1)\cdot T}$$

Then, considering the usual analysis with zero initial conditions $I_L(0) = 0$:

$$\mathcal{L}\{1-\delta(t)\cdot I_L(t)\}(s) = Z\{I_L(t)\}(z)\cdot\frac{(z^{-D}-z^{-1})}{s} + \\ -\frac{(V_{in}-V(D))}{L\cdot s^2}\cdot\sum_{k=0}^{\infty}\left(z^{-(K+1)} - z^{-K}\cdot z^{-D}\right)$$

Finally, rearranging terms and simplifying:

$$\mathcal{L}\{1-\delta(t)\cdot I_L(t)\}(s) = \left(\frac{z-z^D}{z^D\cdot(z-1)}\right)\cdot \\ \cdot\left(Z\{I_L(t)\}(z) + \frac{(V_{in}-V(D))\cdot T\cdot z}{L\cdot(z-1)^2}\right) \quad (7)$$

4.2 $\boldsymbol{v_o(s)}$

The output equations (5) yields:

$$\begin{cases} \mathcal{L}\{v_o(t)\}(s) = \sum_{K=0}^{\infty} \int_{(K+D)\cdot T}^{(K+1)\cdot T} e^{-s\cdot t} \cdot \\ \cdot \left(e^{-a\cdot t} \left(v_o(0) - \frac{V(D)}{\frac{R_D}{R_L}+1} \right) + \frac{V(D)}{\frac{R_D}{R_L}+1} \right) + \\ +V(D) \cdot \sum_{K=0}^{\infty} \int_{K\cdot T}^{(K+D)\cdot T} e^{-s\cdot t} \cdot e^{-\frac{1}{R_L\cdot C}t} \\ a = \left(\frac{1}{R_L} + \frac{1}{R_D}\right) \cdot \frac{1}{C} \end{cases}$$

Following the same methodology as for $I_L(t)$:

$$\begin{cases} \mathcal{L}\{v_o(t)\}(s) = \\ = -\sum_{K=0}^{\infty} \left(A \cdot \frac{e^{-(s+a)\cdot t}}{s+a} \Big|_{(K+D)\cdot T}^{(K+1)\cdot T} + \right. \\ \left. -\frac{B}{s} \cdot e^{-s\cdot t} \Big|_{(K+D)\cdot T}^{(K+1)\cdot T} \right) + \\ -V(D) \cdot \sum_{K=0}^{\infty} \frac{e^{-(s+\frac{1}{R_L\cdot C})\cdot t}}{s+\frac{1}{R_L\cdot C}} \Big|_{K\cdot T}^{(K+D)\cdot T} \\ a = \left(\frac{1}{R_L} + \frac{1}{R_D}\right) \cdot \frac{1}{C} \end{cases}$$

Where $A = v_o(0) - \frac{V(D)}{\frac{R_D}{R_L}+1}$ and $B = \frac{V(D)}{\frac{R_D}{R_L}+1}$.

Rearranging terms:

$$\begin{cases} \mathcal{L}\{v_o(t)\}(s) = \\ = -A \cdot \sum_{K=0}^{\infty} \left(e^{-s\cdot(K+1)\cdot T} \cdot \frac{e^{-a\cdot(K+1)\cdot T}}{s+a} + \right. \\ \left. -e^{-s\cdot(K+D)\cdot T} \cdot \frac{e^{-a\cdot(K+D)\cdot T}}{s+a} \right) \\ -\frac{B}{s} \cdot \sum_{K=0}^{\infty} \left(e^{-s\cdot(K+1)\cdot T} - e^{-s\cdot(K+D)\cdot T} \right) + \\ -V(D) \cdot \sum_{K=0}^{\infty} \frac{\left(e^{-(s+\frac{1}{R_L\cdot C})\cdot(K+D)\cdot T} - e^{-(s+\frac{1}{R_L\cdot C})\cdot K\cdot T} \right)}{s+\frac{1}{R_L\cdot C}} \\ a = \left(\frac{1}{R_L} + \frac{1}{R_D}\right) \cdot \frac{1}{C} \end{cases}$$

As for $I_L(t)$, in order to collect a Z-transform expression, the repalcement $e^{s\cdot T} = z$ leads:

$$\begin{cases} \mathcal{L}\{v_o(t)\}(s) = \\ -\frac{A}{(s+a)} \cdot \left(\frac{z^{-1} \cdot e^{-a\cdot T}}{1 - z^{-1} \cdot e^{-a\cdot T}} - \frac{z^{-D} \cdot e^{-a\cdot D\cdot T}}{1 - z^{-1} \cdot e^{-a\cdot T}} \right) + \\ -\frac{B}{s} \left(\frac{z^{-1}}{1-z^{-1}} - \frac{z^{-D}}{1-z^{-1}} \right) - V(D) \cdot \left(\frac{1}{s+\frac{1}{R_L\cdot C}} \right) \cdot \\ \cdot \left[\frac{(z \cdot e^{\frac{T}{R_L\cdot C}})^{-D}}{1 - z^{-1} \cdot e^{-\frac{T}{R_L\cdot C}}} - \frac{1}{1 - z^{-1} \cdot e^{-\frac{T}{R_L\cdot C}}} \right] \\ a = \left(\frac{1}{R_L} + \frac{1}{R_D}\right) \cdot \frac{1}{C} \end{cases}$$

To simplify the analysis, we can recall the Assumption 1:

$$(K + D) \cdot T \sim K \cdot T \quad (T \to 0)$$

In this way:

$$\mathcal{L}\{v_o(t)\}(s) = -\frac{A}{s+a} \left(\frac{z^D \cdot e^{-a\cdot T} - z \cdot e^{-a\cdot D\cdot T}}{z^D \cdot (z - e^{-a\cdot T})} \right) - \frac{B}{s} \cdot \left(\frac{z^D - z}{z^D \cdot (z-1)} \right) \quad (T \to 0)$$

Considering the transformation:

$$\begin{cases} \frac{1}{s+a} = \frac{z}{z - e^{-a\cdot T}} \\ \frac{1}{s} = \frac{z}{z-1} \end{cases}$$

Finally:

$$\mathcal{L}\{v_o(t)\}(s) = -\frac{A\cdot z}{z-e^{-a\cdot T}} \left(\frac{z^D \cdot e^{-a\cdot T} - z\cdot e^{-a\cdot D\cdot T}}{z^D \cdot (z-e^{-a\cdot T})} \right) - \frac{B\cdot z}{(z-1)} \cdot \left(\frac{z^D - z}{z^D \cdot (z-1)} \right) \tag{8}$$

4.3 Complete Transfer's Function

The electrical circuit's equations (4]) along with (7) and (8) leads:

$$\begin{cases} \left(\frac{z-z^D}{z^D\cdot(z-1)} \right) \cdot \left(Z\{I_L(t)\}(z) + \frac{(V_{in}-V(D))\cdot T\cdot z}{L\cdot(z-1)^2} \right) = \\ = \left[-\frac{A\cdot z}{z-e^{-a\cdot T}} \left(\frac{z^D\cdot e^{-a\cdot T} - z\cdot e^{-a\cdot D\cdot T}}{z^D\cdot(z-e^{-a\cdot T})} \right) + \right. \\ \left. -\frac{B\cdot z}{(z-1)} \cdot \left(\frac{z^D - z}{z^D\cdot(z-1)} \right) \right] \cdot \left(C \cdot s + \frac{1}{R_L} \right) \\ a = \left(\frac{1}{R_L} + \frac{1}{R_D}\right) \cdot \frac{1}{C} \\ B = \frac{1}{\frac{R_D}{R_L}+1} \end{cases} \tag{9}$$

Where $I_L(z) = Z\{I_L(t)\}(z)$. In the next section, the main results will be presented obtaining both: a simplified asymptotic transfer function and a stability theorem to ensure stability for $\forall D \in [0,1]$.

5 Main Results

The Boost converter along with its dynamical model in z-transform (9), can be represented as a transfer function in the Z domain:

$$I_L(z) = \left(\frac{z^D \cdot (z-1)}{(z-z^D)}\right) \cdot$$
$$\cdot \left[-\frac{A \cdot z}{z-e^{-a \cdot T}}\left(\frac{z^D \cdot e^{-a \cdot T} - z \cdot e^{-a \cdot D \cdot T}}{z^D \cdot (z-e^{-a \cdot T})}\right) + \right.$$
$$\left. -\frac{B \cdot z}{(z-1)} \cdot \left(\frac{z^D - z}{z^D \cdot (z-1)}\right)\right] \cdot$$
$$\cdot \left(C \cdot s + \frac{1}{R_L}\right) - \left(\frac{(V_{in} - V(D)) \cdot T \cdot z}{L \cdot (z-1)^2}\right)$$

For the purpose of collecting a complete expression in the domain of z:

$$I_L(z) = \left(\frac{z^D \cdot (z-1)}{(z-z^D)}\right) \cdot$$
$$\cdot \left[-\frac{A \cdot z}{z-e^{-a \cdot T}}\left(\frac{z^D \cdot e^{-a \cdot T} - z \cdot e^{-a \cdot D \cdot T}}{z^D \cdot (z-e^{-a \cdot T})}\right) - \frac{B \cdot z}{(z-1)} \cdot \left(\frac{z^D - z}{z^D \cdot (z-1)}\right)\right] \cdot$$
$$\cdot C \cdot \left(\frac{z - e^{-\frac{T}{R_L \cdot C}}}{z}\right) - \left(\frac{(V_{in} - V(D)) \cdot T \cdot z}{L \cdot (z-1)^2}\right) \quad (10)$$

Then, considering the asymptotic behavior of $I_{L(t)}$ when the sample's number K tends to infinity,[11]:

$$limit_{K \to \infty} I_L(K \cdot T) = lim_{z \to 1}(z-1) \cdot I_L(z) =$$
$$= lim_{z \to 1}(z-1) \cdot \left(\frac{z^D \cdot (z-1)}{(z-z^D)}\right) \cdot$$
$$\cdot \left[-\frac{A \cdot z}{z-e^{-a \cdot T}}\left(\frac{z^D \cdot e^{-a \cdot T} - z \cdot e^{-a \cdot D \cdot T}}{z^D \cdot (z-e^{-a \cdot T})}\right) + \right.$$
$$\left. -\frac{B \cdot z}{(z-1)} \cdot \left(\frac{z^D - z}{z^D \cdot (z-1)}\right)\right] \cdot$$
$$\cdot C \cdot \left(\frac{z - e^{-\frac{T}{R_L \cdot C}}}{z}\right) - \left(\frac{\left(V_{in} - V(D)\right) \cdot T \cdot z}{L \cdot (z-1)^2}\right) =$$
$$= lim_{z \to 1} - \frac{(V_{in} - V(D)) \cdot T \cdot z}{L \cdot (z-1)} \to \infty$$

Then it is clear that, asymptotically, the dominating part of the transfer function (10) is ([12], [13]):

Theorem 1: Given the z-transfer's function (10), an asymptotic equivalent transfer function is as follows:

$$I_L(z) = -\frac{(V_{in} - V(D)) \cdot T \cdot z}{L \cdot (z-1)} \quad (K \to \infty) \quad (11)$$

As a consequence, the next corollary shows a sufficient condition for stability allowing the available LTI stability tools:

Corollary 1: Given the transfer's function (11), the complete closed-loop system, after some controller's addition, will be asymptotically stable if is asymptotically stable for $\forall D \in [0,1]$.

Proof 1: Considering that the duty D changes over time but onyl from interval to interval: $[K \cdot T, (K+1) \cdot T]$, then if for every D, the closed-loop system is stable, each interval is decreasing exponentially (LTI system) and so, because of the inductor's current $I_L(t)$ continuity (either for continuos or discontinuous modes), the current will set to zero or continues from the previous state in previous switching, the complete current evolution over time is decreasing to some equilibrium, so asymptotic stability is proved. This completes the proof.

It is worth noticing that Corollary 1 allows the use of any LTI stability criteria as long as is applied for the complete range $D \in [0,1]$.

Using these results, the next section presents the design of a Lead compensator for the closed-loop stability of the Boost converter.

6 Sensitivity and Error Analysis

According to model (10) and its asymptotic approximation (11), the following analysis can be depicted:

- Analyses of sensitivity: An analysis of the asymptotic transfer function's parameter dependence is not difficult:

$$I_L(z) = -\frac{(V_{in} - V(D)) \cdot T \cdot z}{L \cdot (z-1)}$$

As the model relies on Assumption 1, it is valid for high frequency switching PWM signals. In contrast, since the inductance value L acts as a gain, it is important to keep it close to reality in order to design a more reliable controller.

- Error analysis: taking into account models (10) and (11), the following error analysis can be carried out:

$$lim_{z\to 1}(z-1)\cdot\left[-\frac{(V_{in}-V(D))\cdot T\cdot z}{L\cdot(z-1)} -\left(\frac{z^D\cdot(z-1)}{(z-z^D)}\right)\cdot\left[-\frac{A\cdot z}{z-e^{-a\cdot T}}\cdot\left(\frac{z^D\cdot e^{-a\cdot T}-z\cdot e^{-a\cdot D\cdot T}}{z^D\cdot(z-e^{-a\cdot T})}\right)+\frac{B\cdot z}{(z-1)}\cdot\left(\frac{z^D-z}{z^D\cdot(z-1)}\right)\right]\cdot C\cdot\left(\frac{z-e^{-\frac{T}{R_L\cdot C}}}{z}\right)+\left(\frac{(V_{in}-V(D))\cdot T\cdot z}{L\cdot(z-1)^2}\right)\right]=$$

$$=-B\cdot C\cdot\left(1-e^{-\frac{T}{R_L\cdot C}}\right)$$

Both models converge as the system runs out under Assumption 1 and for small values of the capacitor C.

7 Other Methods Comparison

7.1 Computational Intelligence

A boost controller can be designed using methods derived from computational intelligence, such as fuzzy logic, without the need for a model or transfer function. As a negative aspect, some knowledge about the boost under study must be provided regarding the case-dependent nature of the method, [14], [15].

Alternatively, it is possible to employ neural networks with some very recent references, [16], in which a controller with nonlinear function based on Back Propagation (BP) neural networks combined with PID is developed. Because the model is never used or derived, it is always necessary to train a neural network, even for simple boost designs without the possibility of determining asymptotic stability. Moreover, even with realistic modeling using real data, training a neural network for every controller design is not advantageous for some control objectives, [17].

7.2 Artificial Intelligence

A genetic algorithm is used in [18], even when a model and backstepping are considered to provide asymptotic stability using Lyapunov's method, an average model is finally utilized with the obvious drawback of linearization and without any universal model (transfer function) as presented in this paper.

In the recent paper [19], a black-box model is presented using real time measurements and a NARX-ANN structure, however, as for the previous analysis, its case-dependent nature and the lack of asymptotic stability tools, make the contribution limited when compared to the universal and non-approximated model in this paper.

7.3 Classical Methods

Boost converters are switching models, so a switching strategy or average (linearized) model can be used to obtain a stabilizing controller (see, for instance [20], and [21]). Several advantages can be enumerated in this paper, including:

- No linearization is involved
- A universal asymptotic model is provided with a very simple structure
- A transfer function in the z-domain with no discrete approximations is presented.

The universal and ready-to-use transfer function is a very important contribution in this paper when compared to the available literature where a case-dependent study must be carried out under a linear and local approximation.

8 Matlab Simulations

8.1 Example 1

In this example, a boost converter with $48V$ in V_{in} and with an expected DC value of $v_o = 311V$ will be considered. Using the simplified transfer function (11) for a boost converter, a lead compensator can be designed starting, for instance, from a root locus plot using a simple proportional controller: $V(D) = K_p = \frac{V_{in}}{1-D} \in [1{,}500]$, with $R_L = 10\Omega$, $C = 100\mu F$, $R_D = 0.1\Omega$, as shown in Figure 4.

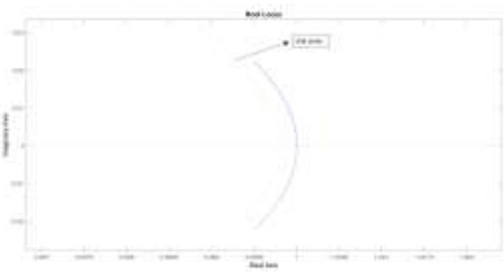

Fig. 4: Root locus for a boost converter with a proportional controller $K_p \in [1V, 500V]$

Where the proportional K_p was considered only for the present real case of $K_p \in [1V, 500V]$. Clearly, as expected, a simple proportional controller can not stabilize a boost converter within this range of K_p. Apllying a lead compensator with $K_p = 311$:

$$G_{lead} = 311 \cdot \frac{z - 0.3}{z - 0.1}$$

Then, the root locus plot is shown in Figure 5. Now the closed-loop system is stable and can be applied to the power systems model in Simulink (Figure 6), where the current $I_L(t)$ versus a set point of 100A is shown in Figure 7. As usual, overpeaks in $V(D)$ internal voltage can be as high as 500V.

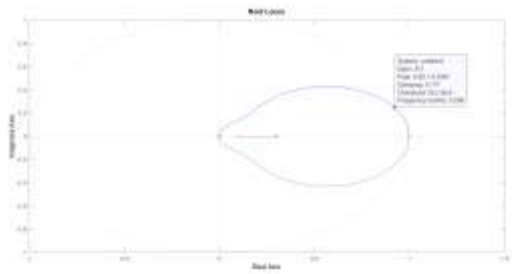

Fig. 5: Root locus for a boost converter with a lead compensator

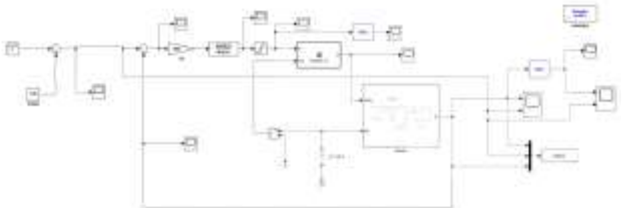

Fig. 6: Boost converter Simulink's model

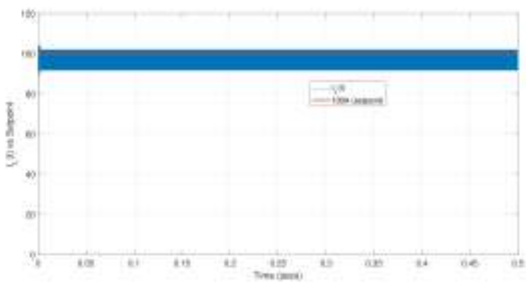

Fig. 7: $I_L(t)$ versus a 100A setpoint

8.2 Example 2

The asymptotic stability analysis in this paper can be also applied to small booost converters, let's say: $5V$ in V_{in} and with and expected DC value of $v_o = 12V$, [22]. Then, the asymptotic transfer's function (11) leads:

$$I_L(z) = -\frac{(1.5 - V(D)) \cdot T \cdot z}{L \cdot (z - 1)} \quad (K \to \infty)$$

For comparison, let's consider the high frequency used in [21]: $T = 2.5\mu s$ and with $L = 10\mu Hy$ for an output power of about $6W$ using $C = 150\mu F$, the following controller stabilizes the DC-DC converter:

$$G_{compensator} = 4 \cdot \frac{z - 0.9958}{z - 0.9739}$$

It turns out that this controller is a z-transform version of the one in [22]. Notice the reduced phase margin due to the discrete conversion when compared to the continuous model (Figure 8).

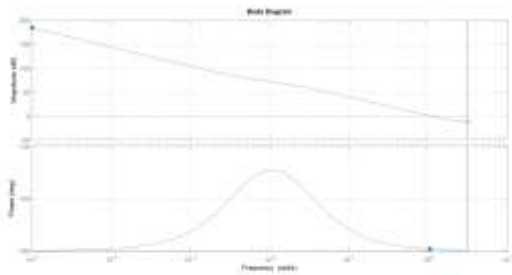

Fig. 8: Bode plot for the compensated boost converter

9 Conclusion

As a result of applying Laplace transforms, the z-transform naturally follows without any local approaches or linearization, rather the switching nature of the model is captured by the z-transform, and the complete model is transformed into a unique transfer function (universal transfer function for any boost converter).

Therefore, all classical tools apply to the design of compensators and stabilizers for boost converters/power converters using the simplified asymptotic transfer function in this paper. Moreover, an interesting new transfer function showed up including terms like z^D deserving a complete separate study. In this paper, an asymptotic model was also derived to provide a simple methodology to design a lead compensator using a universal discrete transfer function.

To validate the analysis, a boost converter was evaluated in Simulink using the Power Systems toolbox showing the asymptotic convergence of the current $I_L(t)$ to some desired setpoint of about 100A (plus ripples) and also a small 5V to 12V (24W) is analyzed and compared with a Texas Instruments' design.

This research opens the door to more convenient and sophisticated models using complementary switching for a wider range of DC-DC and also DC-AC converters, which comprises a complete future research line. The universal structure of the asymptotic transfer, which facilitates asymptotic stability, renders the utilization of these strategies highly appealing.

As future work, more DC-DC converters will be explored with the ideas presented in this paper along with real cases and test measurements.

Acknowledgement:
The authors would like to acknowledge Universidad Tecnológica Nacional, Departamento de Ingeniería Eléctrica, and GESE.

References:
[1] Al-Baidhani, H.; Corti, F.; Reatti, A.; Kazimierczuk, M.K. Robust Sliding-Mode Control Design of DC-DC Zeta Converter Operating in Buck and Boost Modes. *Mathematics*, vol. 11, Issue 3791, 2023, https://doi.org/10.3390/math11173791.
[2] Brian T. Lynch. *Under the Hood of a DC/DC Boost Converter*. Texas Instruments.
[3] A. P. Podey and J. O. Chandle. Stability Analysis of DC-DC Boost Converter using Sliding Mode Controller. *IEEE PES/IAS* PowerAfrica, Nairobi, Kenya, pp. 1-5, 2020, 10.1109/PowerAfrica49420.2020.9219954.
[4] Praful V. Nandankar and Prashant P. Bedekar and Prashantkumar V. Dhawas. Efficient DC-DC converter with optimized switching control: A comprehensive review. Sustainable Energy Technologies and Assessments, vol. 48, pp. 101670. 2021, https://doi.org/10.1016/j.seta.2021.101670.
[5] M. di Bernardo, C. J. Budd, A. R. Champneys, P. Kowalczyk. *Piecewise-smooth dynamical systems: theory and applications*. Springer. 2008.
[6] R. D. Middlebrook and S. Cuk. A general unified approach to modeling switching converter stages. *IEEE Power Electronics Specialists Conf.*, pp. 18-34, 1976.
[7] C. T. Rim, G. B. Joung and G. H. Cho. A state-space modeling of nonideal DC-DC converters. PESC '88 Record., *19th Annual IEEE Power Electronics Specialists Conference*, Kyoto, Japan, vol.2, pp. 943-950. 1988. doi: 10.1109/PESC.1988.18229.
[8] Marey, A.; Bhaskar, M.S.; Almakhles, D.; Mostafa, H. Analytical Solution for Transient Reactive Elements for DC-DC Converter Circuits. Electronics, vol 11, issue 3121, 2022, https://doi.org/10.3390/electronics11193121.
[9] Anup Marahatta and Yaju Rajbhandari and Ashish Shrestha and Sudip Phuyal and Anup Thapa and Petr Korba. Model predictive control of DC/DC boost converter with reinforcement learning. Heliyon, Vol. 8, issue 11, pp. 1-13, 2022, https://doi.org/10.1016/j.heliyon.2022.e11416.
[10] Sanakhan, Safoora and Mahery, H. Mashinchi and Babaei, E. and Sabahi, M. Stability Analysis of Boost DC-DC Converter Using Z-Transform. *IEEE 5th India International Conference on Power Electronics (IICPE)*, pp: 1-6, 2012. 10.1109/IICPE.2012.6450432.
[11] Charles Phillips and Troy Nagle. *Digital Control System Analysis and Design*. Pearson, 3th Edition. 2014.
[12] N. G. de Bruijn, *Asymptotic Methods in Analysis*. Dover ed Edition. 2010.
[13] D. Murray. *Asymptotic analysis: (Applied Mathematical Sciences, 48)*. Springer; Reprint edition. 1984.
[14] R. J. Wai, M. W. Chen and Y. K. Liu. Design of Adaptive Control and Fuzzy Neural Network Control for Single-Stage Boost Inverter. *IEEE Transactions on Industrial Electronics*, Vol. 62, issue 9, pp. 5434-5445, 2015, doi: 10.1109/TIE.2015.2408571.
[15] S. Chimplee and S. Khwan-On, Fuzzy Controller Design for Boost Converter Based on Current Slope. *2022 International Electrical Engineering Congress (iEECON)*, Khon Kaen, Thailand, pp: 1-4, 2022, 10.1109/iEECON53204.2022.9741597.
[16] H. Xi and Q. Wang, Design of Back Propagation Neural Network PID Control for Boost Converter. *IEEE Sustainable Power and Energy Conference (iSPEC)*, Nanjing, China, pp. 3889-3893, 2021, 10.1109/iSPEC53008.2021.9735583.
[17] O. Asvadi-Kermani, B. Felegari, H. Momeni, S. A. Davari and J. Rodriguez. Dynamic Neural-Based Model Predictive Voltage Controller for an Interleaved Boost Converter With Adaptive Constraint Tuning. *IEEE Transactions on Industrial Electronics*, vol. 70, no. 12, pp. 12739-12751, 2023, doi: 10.1109/TIE.2023.3234138.
[18] I. A. Ayad, E., Elmostafa, A. Umaid, Q. Saeed, W. Asad, B. Mohamed and A. Ahmad. Optimized Nonlinear Integral Backstepping Controller for DC–DC Three-Level Boost Converters. *IEEE Access*, Vol. 11, pp. 49794-

49805, 2023, 10.1109/ACCESS.2023.3274773.

[19] A. Zilio, D. Biadene, T. Caldognetto and P. Mattavelli. Black-Box Large-Signal Average Modeling of DC-DC Converters Using NARX-ANNs. *IEEE Access*, vol. 1, pp. 43257-43266, 2023. doi: 10.1109/ACCESS.2023.3271731.

[20] Ahmed Chouya. Adaptive Linearizing Control with MRAC Regulator for DC-DC Boost Converter. *International Journal on Applied Physics and Engineering*, vol. 1, pp. 25-30, 2022, doi:10.37394/232030.2022.1.4.

[21] M. Cherif Daia Eddine Oussama, C. Ali, K. Abdelhalim. Robust Integral Linear Quadratic Control for Improving PV System Based on Four Leg Interleaved Boost Converter. *WSEAS Transactions on Systems*, vol. 21, pp. 39-48, 2022, https://doi.org/10.37394/23202.2022.21.4.

[22] AN-1994 Modeling and Design of Current Mode Control Boost Converters. Application Report SNVA408B, Texas Instruments, 2013, [Online]. https://www.ti.com/lit/an/snva408b/snva408b.pdf?ts=1710084702459 (Accessed Date: March 1, 2024).

Contribution of Individual Authors to the Creation of a Scientific Article (Ghostwriting Policy)

The authors equally contributed in the present research, at all stages from the formulation of the problem to the final findings and solution.

No funding was received for conducting this study.

Sources of Funding for Research Presented in a Scientific Article or Scientific Article Itself

No funding was received for conducting this study.

Conflict of Interest

The authors have no conflicts of interest to declare.